The ^3He spin-dependent structure functions within the Light-front Hamiltonian Dynamics

Author:
Eleonora Proietti (PG),
from November in Pisa

In collaboration with:
Filippo Fornetti (PG)
Emanuele Pace (RM)
Matteo Rinaldi (PG)
Giovanni Salmè (RM)
Sergio Scopetta (PG)

Outline

Calculation of spin-dependent structure functions (SSFs) g_1 and g_2 for the ^3He nucleus:

- Polarized Deep Inelastic Scattering (DIS)
- Polarized ^3He target
- The Light-Front Dynamics (LF)
- Spin dependent structure functions g_1 and g_2
- Numerical calculation of the SSFs
- Extraction of the neutron SSFs

Deep Inelastic Scattering (DIS)

$$l(\ell) + N(P) \to l'(\ell') + X(P_X),$$

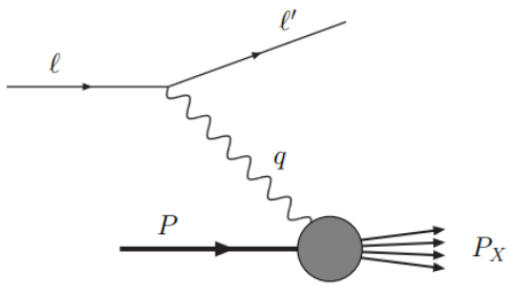

Figure 1: DIS [1]

Deep Inelastic Scattering
(DIS) is an inelastic scattering process between
a lepton and a high-energy hadron, where the hadron
breaks up and is not detected in the final state.

In the laboratory frame: $q = (\nu, 0, 0, -q)$
In the Bjorken limit: $\nu \to \infty$, $Q^2 = -q^2 \to \infty$,
while $x = \frac{Q^2}{2M\nu}$ is fixed.

Infintum Momentum Frame:
the proton and the virtual photon
are collinear (along the z-axis),
and the proton has infinite momentum ($p_z \to \infty$).

[1] Barone A, Drago A and Ratcliffe P, Phys. Rept. **359** 1-168 (2002).

Process under the investigation: scattering of polarized electrons e^- on a polarized nucleon $N \rightarrow$ like the ^3He nucleus, with spin 1/2.

Differential cross-section:

$$\frac{d\sigma}{dE'd\Omega} = \frac{\alpha_{em}^2}{2MQ^4}\frac{E'}{E}[L^s_{\mu\nu}W^{\mu\nu\ s} + L^a_{\mu\nu}W^{\mu\nu\ a}].$$

Antisymmetric part of the hadronic tensor for a nucleus with A nucleons:

$$W^a_{A\mu\nu} = \frac{2M\epsilon_{\mu\nu\rho\sigma}q^\rho}{P\cdot q}S^\sigma g_1(x,Q^2) + \left[S^\sigma - \frac{S\cdot q}{P\cdot q}P^\sigma\right]g_2(x,Q^2).$$

Extraction of SSFs g_1 and g_2 from $W^a_{A\mu\nu}$:

$$g_j^A(x,Q^2) \ = (-1)^j \ \frac{i\ \nu}{2|\boldsymbol{q}|}\left[\frac{Q^2}{|\boldsymbol{q}|^2}\frac{W^a_{A,02}}{S_x} - \frac{\nu}{|\boldsymbol{q}|}\frac{W^a_{A,12}}{S_z}\frac{W^a_{A,02}}{S_x}\frac{1+(-1)^j}{2}\right],$$

with $j = 1, 2$.

Open issues

We recall that for the EMC effect (see Rinaldi's talk):

- NR calculations: qualitatively in agreement with the results but do not satisfy the baryon number sum rule and the momentum sum rule (MSR) at the same time.
- Relativistic light front calculation: the best conventional evaluation because it fulfills both the sum rules at the same time.

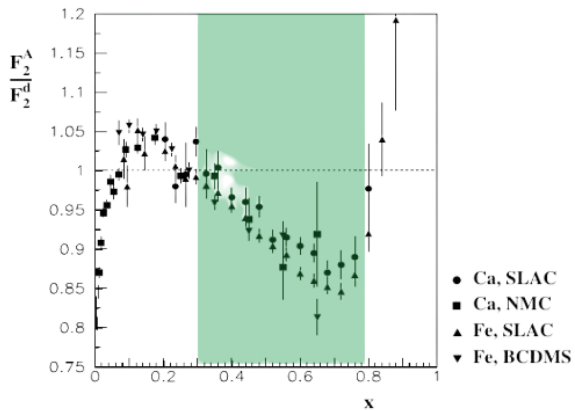

Figure 2: Effetto EMC.

Promising results for the ^3He [2]:
we apply the approach to the polarized case.

[2] E. Pace, M. Rinaldi, G. Salmè, and S. Scopetta, Phys. Letters B 839, 137810 (2023).

The ^3He target

We start with ^3He:

- An interesting "laboratory" for studying the general properties of a three-body system with spin 1/2.
- Experimentally, one of the future tasks of the EIC [3] is the study of DIS processes with both polarized and unpolarized ^3He.
  High energies: relativity could be important.
- Theoretically, it is possible to derive a wave function for ^3He by using phenomenological potentials.
- The polarization of ^3He is very close to the one of the neutron, approximately 90%, with realistic potentials → this makes the ^3He an effective neutron target.

Magnetic momentum: neutron $-1.91\ \mu_N$, ^3He $-2.128\mu_N$

[3] R. Abdul Khalek, et al., Nucl. Phys. A 1026 122447, (2022).

We summarize the LF Hamiltonian dynamics framework (LFHD)

Relativistic quantum mechanics → we need the Poincaré covariance.

Dirac introduced various models of relativistic dynamics in his 1949 work, including the Light-Front with the initial condition: $x^+ = 0$.

Light-cone coordinates (used in LF):

$$x^\mu = (x^0, x^1, x^2, x^3) \to (x^-, x^+, \mathbf{x}_\perp) = (x^-, \tilde{x}), \quad \text{con } \mathbf{x}_\perp = (x_1, x_2)$$
$$x^+ = x^0 + x^3, \qquad x^- = x^0 - x^3.$$

Scalar product: $x \cdot y = \frac{1}{2}[x^+ y^- + x^- y^+] - \mathbf{x}_\perp \mathbf{y}_\perp$.

Boosts and rotations LF: $\mathbf{E}_\perp = \mathbf{K}_\perp + \hat{z} \times \mathbf{J}_\perp, \quad \mathbf{F}_\perp = \mathbf{K}_\perp - \hat{z} \times \mathbf{J}_\perp,$

Advantages of the LFHD:

- Maximum number of kinematic generators: 7, including boosts and P^+: their eigenvalues are conserved in an interacting system.

- The description of DIS in the IMF is straightforward.

- Bakamjiam-Thomas (BT) construction:

  A method to construct Poincaré group generators in an interacting system while preserving covariance [4].

  - Only the mass operator M contains the interaction,
  - M generates the interaction dependence in P^-

  The BM mass operator can be approximated as the NR mass operator but in a covariant approach: $M_{BT} \sim M^{NR}$.

  Invariant under rotations and translations.

[4] B. Bakamjian and L. H. Thomas, ii. Phys. Rev., 92:1300–1310, (1953).

LF dynamics for an interacting system

Minus component of momentum (for on-shell particles):

$$p_i^- = \frac{m_i^2 + |\mathbf{p}_{i\perp}|^2}{p_i^+},$$

intrinsic variables, they do not depend on the absolute motion of the system and are invariant under Light-Front boosts:

$$\xi_i = \frac{p_i^+}{P^+}, \quad \mathbf{k}_{i\perp} = \mathbf{p}_{i\perp} - \frac{p_i^+}{P^+}\mathbf{P}_\perp = \mathbf{p}_{i\perp} - \xi_i \mathbf{P}_\perp.$$

where: p_i^+ is the momentum of the nucleon, P^+ is the momentum of the nucleus and ξ_i is the fraction of the momentum of the nucleus carried by the nucleon.
The total LF momentum of the system is conserved and is given by:

$$P^+ = \sum_{i=1,n} p_i^+, \quad \mathbf{P}_\perp = \sum_{i=1,n} \mathbf{p}_{i\perp}, \rightarrow \sum_i \xi_i = 1, \quad \sum_i \mathbf{k}_{i\perp} = 0.$$

M_0 is the free mass, invariant under boost LF:

$$M_0(1,2,3) = \sum_i \sqrt{m_i^2 + k_i^2} = \sqrt{\sum_i \frac{m_i^2 + |\mathbf{k}_{i\perp}|^2}{\xi_i}}.$$

Hadronic tensor in the LF dynamics

Inclusive scattering of electrons on a nucleus with A nucleons:

$$W_A^{\mu\nu}(P_A, \mathbf{S}, \mathcal{M}, T_{Az}, q) = \frac{1}{2\pi} \sum_X {}_{LF}\langle \Psi_0; \mathbf{S}, \mathcal{M}, T_{Az}; P_A | J_A^\mu(0) | X, P_X \rangle_{LF}$$
$$\times {}_{LF}\langle X, P_X | J_A^\nu(0) | \Psi_0; \mathbf{S}, \mathcal{M}, T_{Az}; P_A \rangle_{LF} \ (2\pi)^4 \ \delta^4(q + P_A - P_X).$$

Impulsive approximation (IA): $J_A^\mu(0) = \sum_N J_N^\mu(0)$.

In IA, the antisymmetric part of the hadronic tensor becomes:

$$W_A^{a,\,\mu\nu} = \sum_{N\sigma\sigma'} \oint d\epsilon \int \frac{d\boldsymbol{\kappa}_\perp \, d\kappa^+}{2 \ (2\pi)^3 \ \kappa^+} \ \frac{1}{\xi} \ \mathcal{P}^N_{\sigma\sigma'}(\tilde{\boldsymbol{\kappa}}, \epsilon, \mathbf{S}, \mathcal{M}) \ w^{a,\,\mu\nu}_{N,\sigma',\sigma}(p, q).$$

where $p^- = P_A^- - P_S^-$ with p: the 4-momentum of the off-shell nucleon.
$w^{\mu\nu}$ is the single-nucleon hadronic tensor and $\mathcal{P}^N_{\sigma\sigma'}$ is the spectral function (SF).

Spectral Function

- The LF SF is based on the overlap:
  ${}_{LF}\langle tT; \alpha, \epsilon; JJ_z; \tau\sigma, \tilde{\kappa}|j, j_z = m; \epsilon^A, \Pi; T_A\, T_{Az}\rangle$, where:

  $|j, j_z = m; \epsilon^A, \Pi; T_A\, T_{Az}\rangle$: eigenstates of a nucleus with A nucleons,

  $|\tilde{\kappa}, \sigma\tau; JJ_z\epsilon, \alpha, Tt\rangle_{LF}$: intrinsic state of the cluster $[1, (A-1)]$.

- Since we don't know how to use the LF states, we connect them to the canonical (IF) states through the so called Melosh rotation.

- Then we apply the construction to relate the latter to the NR states.

- We can relate the unpolarized spectral function to the spin-dependent one[5]:

$$\mathcal{P}^{\tau}(\tilde{\boldsymbol{\kappa}}, \epsilon) = \frac{1}{2\,j+1} \sum_{m} \sum_{\sigma} \mathcal{P}^{\tau, m, m}_{\sigma\sigma}(\tilde{\boldsymbol{\kappa}}, \epsilon, \hat{z}).$$

- In the end, the calculation is based on the use of the NR realistic wave function.

[5] R. Alessandro, A. Del Dotto, E. Pace, G. Perna, G. Salmè, S. Scopetta, Phys. Rev. C 104 (6) (2021) 065204.

Spin-dependent structure functions (SSFs)

We extract the SSFs g_1 and g_2 from the hadronic tensor $W^{\mu\nu}$

$\longrightarrow$ we can relate the nuclear SSFs to the single nucleon SSFs in the Bjorken limit, through the convolution relationship:

$$g_i^3(x) = \frac{m}{M_3} \sum_{N=n,p} \int_{xm/M_3}^{1} \frac{d\xi}{\xi^2} \mathcal{L}_N(\xi)\, g_i^N(z) \;=\; g_i^{3,n} + 2\, g_i^{3,p}$$

with $z = xm/(M_3\xi)$ e $i = 1, 2$.

g_i^N: SSFs of the free nucleon,

$\mathcal{L}_\mathcal{N}$: light-front spin-dependent momentum distribution with takes into account nuclear effects. This quantity is obtained by properly integrating the SF.

Numerical integrations were performed using Fortran. Ingredients:

- the ^3He wave function (WF) provided by A. Kievsky e M. Viviani [6] obtained from the Argonne v_{18} potential (AV18) [7].
- The free nucleon SSFs of Ref. [8], [9].

---

[6] A. Kievsky, S. Rosati, M. Viviani, Nucl. Phys. A **551**, 241-254, (1993).
[7] R. B. Wiringa, V. G. J. Stoks, R. Schiavilla, (1995).
[8] M. Glück, E. Reya, M. Stratmann, W. Vogelsang, Phys. Rev. D 63, 094005 (2001).
[9] A. Harindranath and Wei-Min Zhang, Phys.Lett. B 408 347-356 (1997).

Polarized LC momentum distributions

$$\mathcal{L}_{\mathcal{N}} : \begin{cases} I^N : & \text{longitudinal pol.} \\ h^N : & \text{traverse pol.} \end{cases}$$

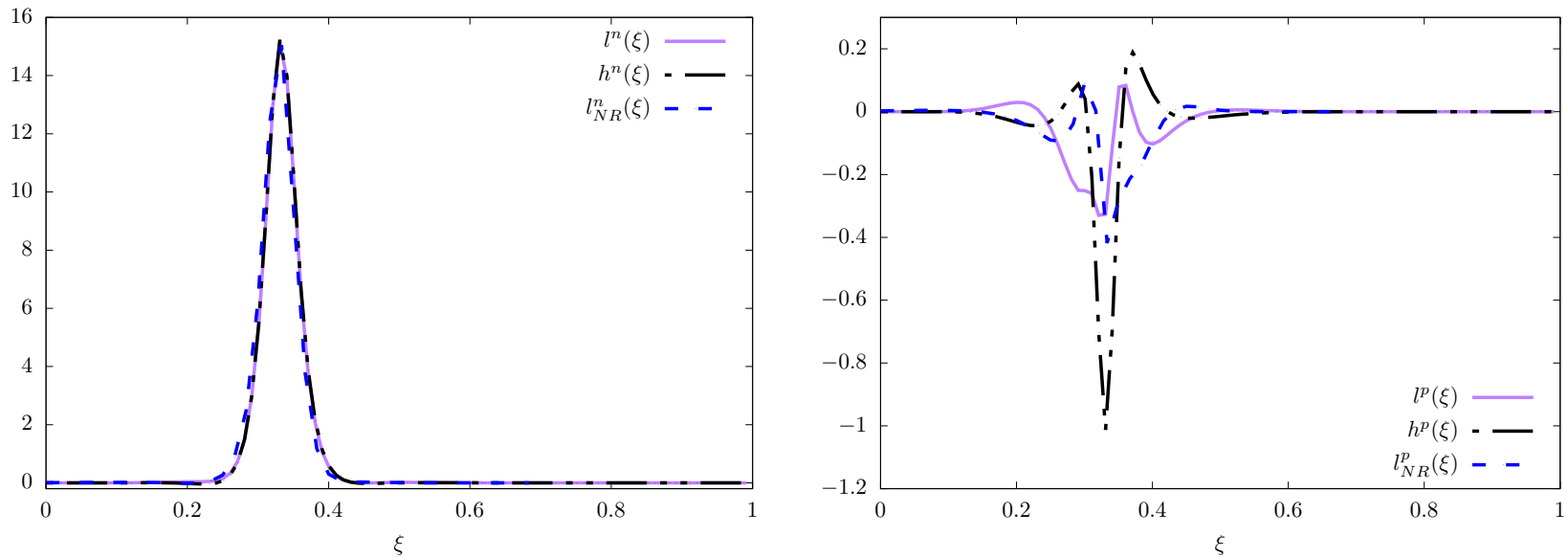

Figure 3: The curves for I^n, h^n, and I^n_{NR} are shown in the left panel. The same for the proton is shown in the right panel [10].

[10] E. Pace, M. Rinaldi, G. Salmè, and S. Scopetta, Phys. Letters B 839, 137810 (2023).

The ^3He SSFs

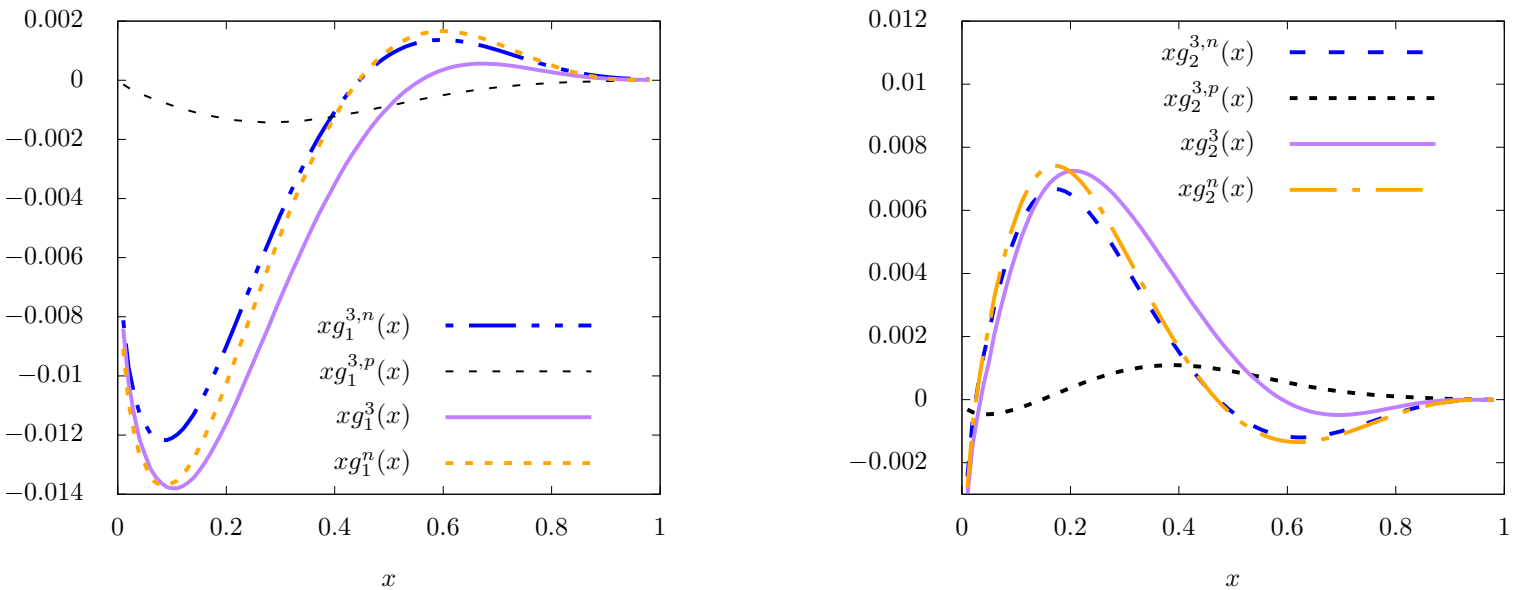

Figure 4: Structure functions $xg_1(x)$ for: ^3He ($xg_1^3(x)$), contribution of the neutron to ^3He ($xg_1^{3,n}(x)$), contribution of the proton to ^3He ($xg_1^{3,p}(x)$), free neutron $xg_1^n(x)$ in the left panel. Same for $xg_2(x)$ in the right panel.

g_1 in the LF case and the NR case

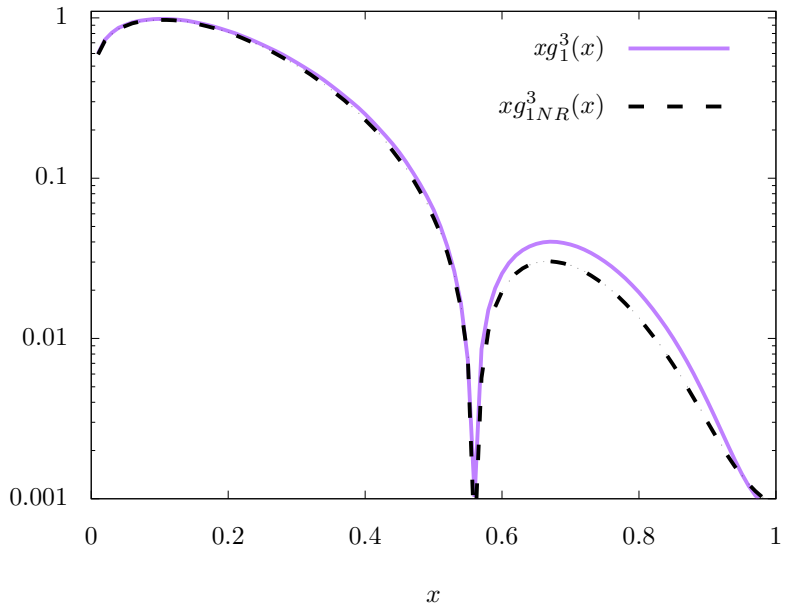

Figure 5: The LF SSF $xg_1^3(x)$ in comparison with the not-relativistic SSF[11] on a logarithmic scale.
The relativistic effects are small and are more significant for large x.

[11] C. Ciofi degli Atti, S. Scopetta, E. Pace, and G. Salmé, Phys. Rev. C *48*, Phys. Rev. C **48**, R968(R) (1993).

Experimental data for the SSFs

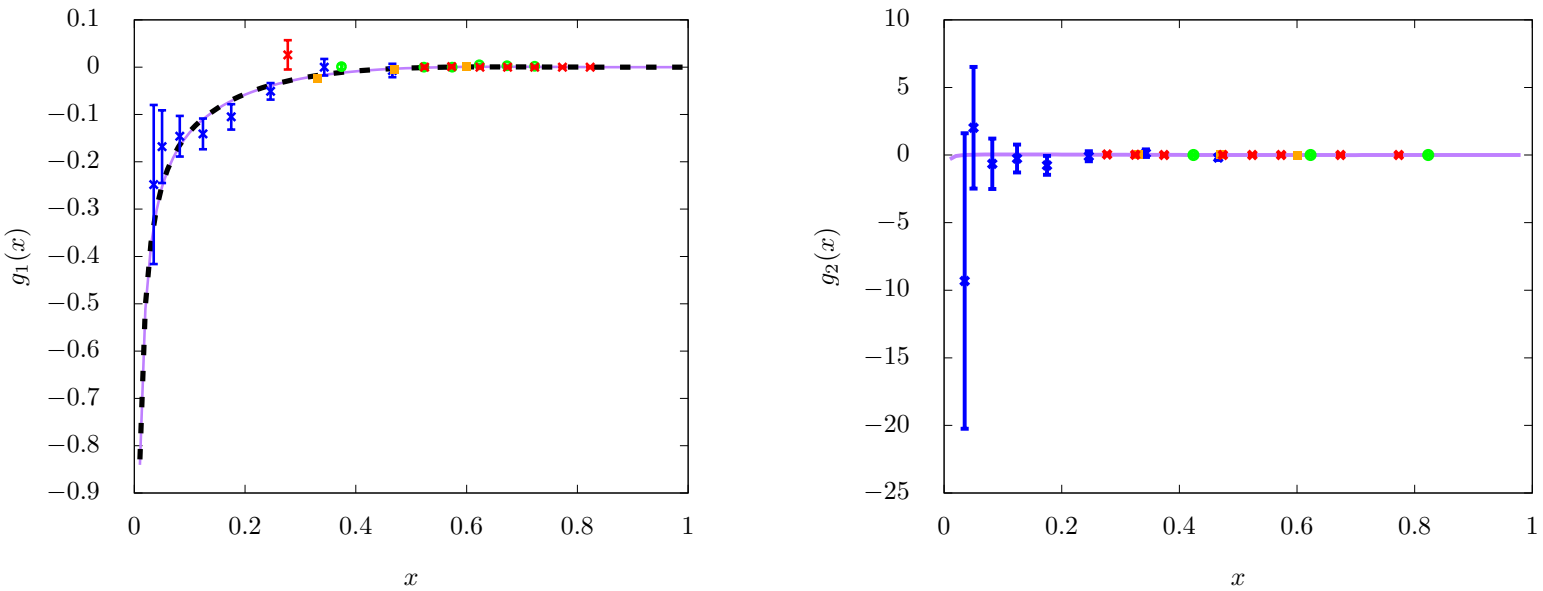

Figure 6: LF SSFs $g_1^3(x)$ (left panel) and $g_2^3(x)$ (right panel) in comparison with the experimental data from E142 [12], JLAB04 [13], and JLAB16 [14].

[12] P. L. Anthony et al. (E142 Collaboration), Phys. Rev. D 54, 6620 (1996).
[13] X. Zheng et al. (Jefferson Lab Hall A Collaboration), Phys. Rev. C 70, 065207 (2004).
[14] D. Flay et al. (Jefferson Lab Hall A Collaboration), Phys. Rev. D 94, 052003 (2016).

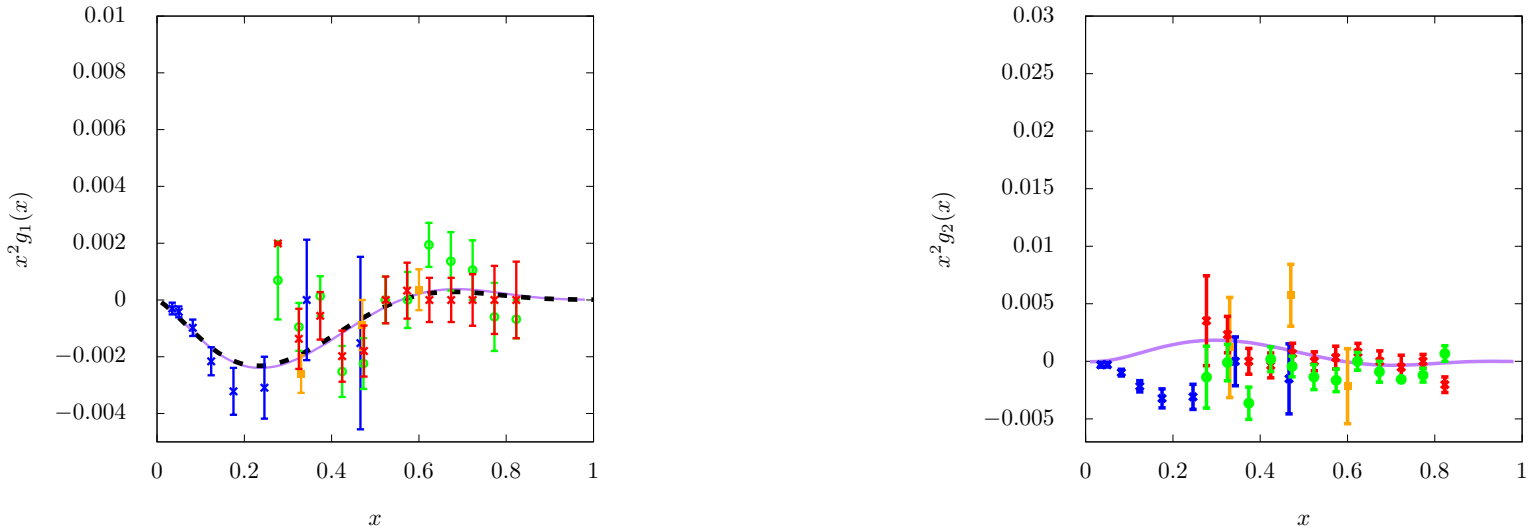

Figure 7: $x^2 g_1^3(x)$ and $x^2 g_2^3(x)$ LF and NR in comparison with the experimental data from E142, JLAB04, and JLAB16 on a logarithmic scale.

- The comparison with the data is excellent.
- There are NO free parameters.
- The calculation is realistic and rigorous (the WF comes from the $av_1 8$ potential).
- For $g_1^3(x)$: The current data do not distinguish the relativistic effects.

Extraction of the neutron SSFs

Since the LF momentum distributions are peaked around $\xi \sim 1/3$, we can approximate g_i^3 as follows:

$$g_1(x) = 2p_p g_1^p(x) + p_n g_1^n(x), \quad g_2(x) = 2t_p g_2^p(x) + t_n g_2^n(x). \tag{1}$$

- $p_n \simeq 0.872$ e $p_p \simeq -0.0228$: effective longitudinal nucleon polarizations
- $t_n \simeq 0.872$ e $t_p \simeq -0.0243$: effective transverse nucleon polarizations.

From this approximation, we extract the SSFs of the neutron from those of the ^3He:

$$\bar{g}_1^n(x) = \frac{1}{p_n}\,[g_1^3(x) - 2p_p\; g_1^{3,p}(x)], \tag{2}$$

$$\bar{g}_2^n(x) = \frac{1}{t_n}\,[g_2^3(x) - 2t_p\; g_2^{3,p}(x)]. \tag{3}$$

Comparison between $g_i^{3,n}$ and g_i^n

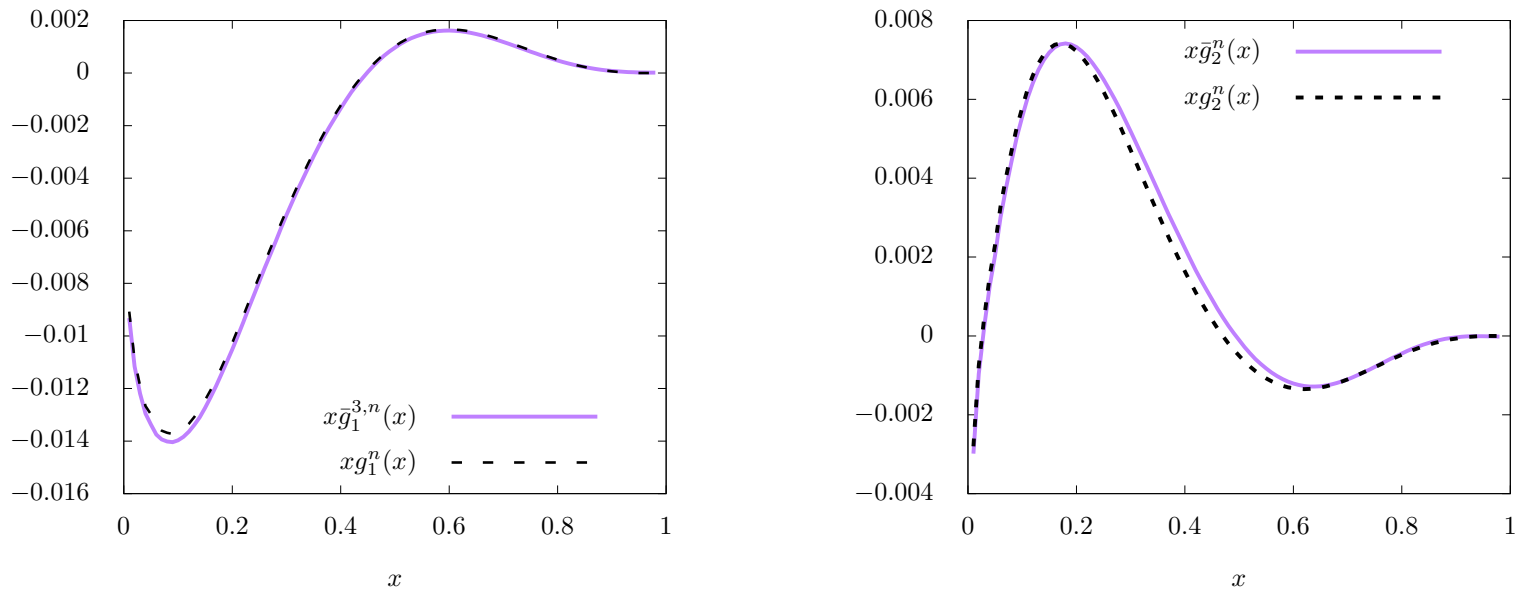

Figure 8: Comparison between $xg_1^n(x)$ of the free neutron and $x\bar{g}_1^n(x)$, in the left panel. Same for $xg_2(x)$ in the right panel.

Conclusions

The numerical results obtained for the SSFs are in line with the expected ones:

- the dominant contribution to the spin distributions of ^3He comes from the neutron,
- the LF SSFs and the NR ones are comparable,
- excellent comparison with data,
- we can approximate the convolution formulas with expressions that allow for the extraction of neutron SSFs by properly taking into account conventional nuclear effects.

Future developments

It will be possible to extend the LF treatment to:

- Exclusive processes to calculate other distributions for ^3He.
- Include interactions in the final state thus going beyond the impulse approximation.

Thanks to this analysis, it will be possible to provide a realistic and relativistic description of the reaction mechanisms for high-energy nuclear processes which are the focus of future experimental programs.

Thanks for the attention!

Backup

Spin-crisis of the proton

We consider the first momentum of g_1:

$$\Gamma_1^{p(n)} \equiv \int_0^1 g_1^{p(n)}(x)dx = \frac{1}{9}\left[\pm\frac{3}{4}g_A^3 + \frac{1}{4}g_A^8 + g_A^0\right],$$

EMC collaboration: measurement of g_1^p and Γ_1^p, using the known values of g_A^3 and g_A^8:

$$g_A^0 \simeq 0,$$

In quark models, the total momentum of the proton derives entirely from the quark spins.

For a quark with flavor q:

$$\langle S_z \rangle = \frac{1}{2}\int_0^1 dx\ \Delta q(x).$$

From which: $g_A^0 = 2\langle S_z^{quarks} \rangle \simeq 0.6$

it is different EMC result for g_A^0 → *Spin-crisis* of the proton → intense experimental and theoretical activity still ongoing.

^3He as effective neutron target

Shell model: spin and parity of ^3He are the same as the unpaired nucleon $J^\pi = \frac{1}{2}^+$.

Magnetic momentum: neutron $-1.91\,\mu_N$, ^3He $-2.128\,\mu_N$

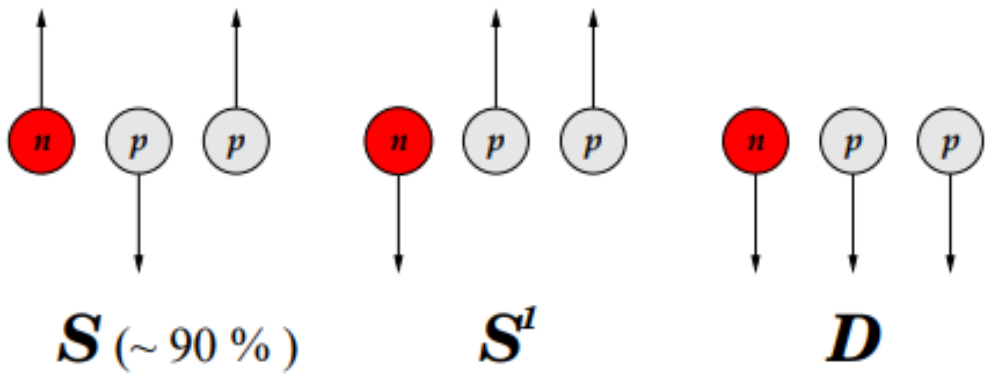

Figure 9: Polarization of neutrons and protons.

Nuclear effects: derives from the waves $\mathcal{S}'$ and $\mathcal{D}$.

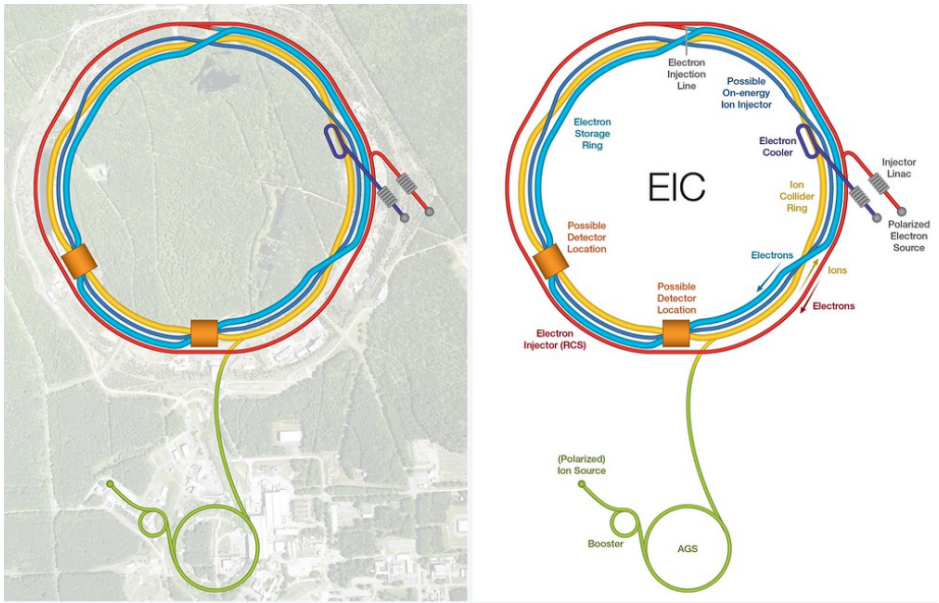

Figure 10: EIC, Brookhaven national laboratory (BNL) Upton, in New York state.

The Electron-Ion Collider consists of two intersecting accelerators: one producing an electron beam, and the other producing a beam of protons or atomic nuclei such as polarized ^3He, which collide at very high energies.

The Nuclear Theory Group of Perugia is a signatory of the "Yellow Report."

Machine parameters:

U.S. 2015 Long-Range Plan for Nuclear Science

- Ion beams: protons, deuterium, ^3He, stable heavy nuclei
- polarization ($\sim 70\%$): electrons, protons, light nuclei (es. ^3He)
- c.m. energy: $\sqrt{s} \sim 20 - 100$ Gev, which can be increased up to ~ 140 Gev
- high luminosity: $\sim 10^{33-34}\ \mathrm{cm}^{-2}\ \mathrm{sec}^{-1}$
- possibility of having more than one interaction region
- high resolution

Why #1

Nucleon mass

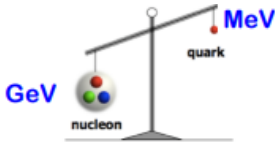

Why #2

proton spin 1/2

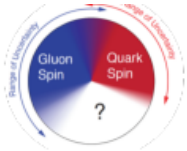

Why #3

hadronization

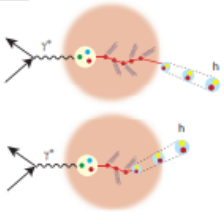

Why #4

gluon saturation

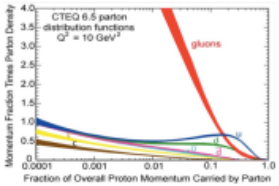

x

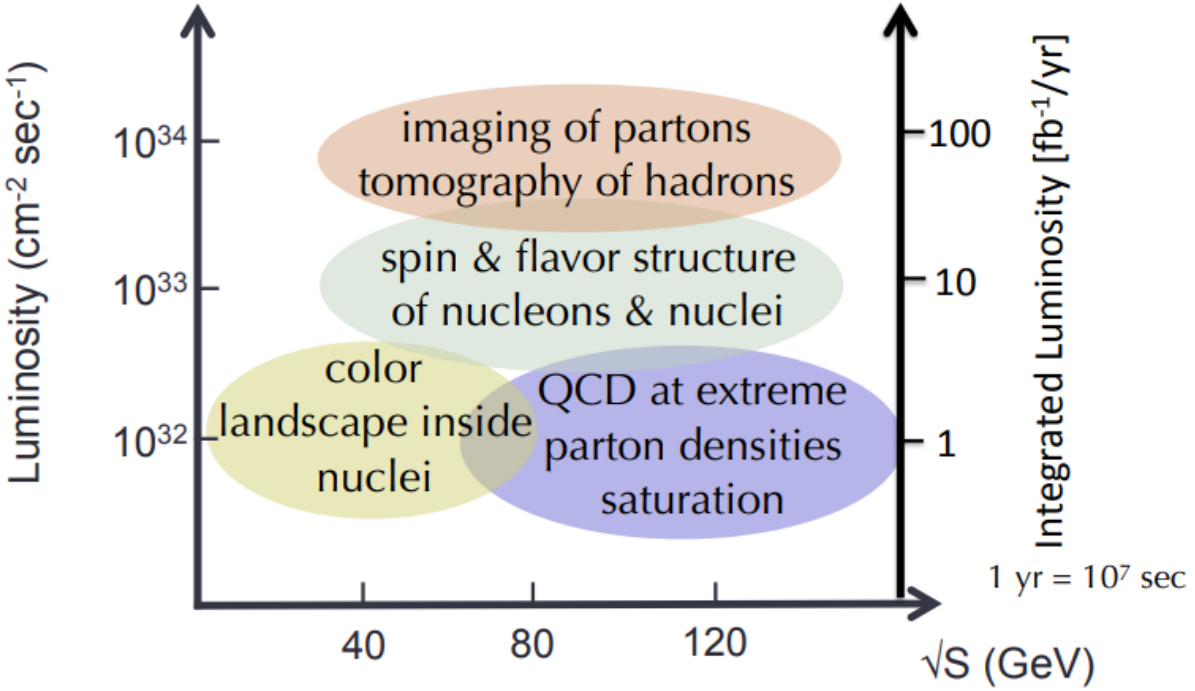

high luminosity and polarization

wide range of c.m. energies and nuclear probes

Intrinsic mass operator with a BT construction:
$M(1,2,3) = M_0(1,2,3) + \mathcal{V}(\mathbf{k}_i \cdot \mathbf{k}_j)$. Three reference frames:

- laboratory frame of the three interacting particles, with total momenta p_i;
- intrinsic LF frame of the three free particles, with momenta k_i;
- intrinsic LF frame of the *cluster*: one free particle and a subsystem of two interacting particles 1+(23), with momenta κ_1 e κ_{23}.

Set of variables for the internal motion of the pair (2,3):

$$\eta = \frac{k_2^+}{k_2^+ + k_3^+} = \frac{\xi_2}{\xi_2 + \xi_3} = \frac{\xi_2}{1 - \xi_1} = \frac{p_2^+}{p_2^+ + p_3^+},$$

$$\mathbf{k}_{23\perp} = \mathbf{k}_{2\perp} - \eta(\mathbf{k}_{2\perp} + \mathbf{k}_{3\perp}) = \mathbf{k}_{2\perp} + \eta\mathbf{k}_{1\perp}, \quad k_{23}^+ = \eta M_{23},$$

where:

$$M_{23}^2 = \frac{m^2 + |\mathbf{k}_{23\perp}|^2}{\eta(1-\eta)} = \left[2\sqrt{m^2 + |\mathbf{k}_{23}|^2}\right]^2.$$

The total LF momentum of the free pair (2,3) in the laboratory frame is:

$$P_{23}^+ = p_2^+ + p_3^+, \qquad \mathbf{P}_{23\perp} = \mathbf{p}_{2\perp} + \mathbf{p}_{3\perp},$$

in the intrinsic three-body frame:

$$K_{23}^+ = k_2^+ + k_3^+, \qquad \mathbf{K}_{23\perp} = \mathbf{k}_{2\perp} + \mathbf{k}_{3\perp} = -\mathbf{k}_{1\perp}.$$

In terms of the nonsymmetric intrinsic variables, the free mass is:

$$M_0(1,2,3) = \sum_{i=1,3} \sqrt{m^2 + |\mathbf{k}_i|^2} = \frac{m^2 + |\mathbf{k}_{1\perp}|^2}{k_1^+} + \frac{M_{23}^2 + |\mathbf{k}_{1\perp}|^2}{K_{23}^+}.$$

$$\mathcal{M}_0^2(1,23) = \frac{m^2 + |\mathbf{k}_{1\perp}|^2}{\xi_1} + \frac{M_S^2 + |\mathbf{k}_{1\perp}|^2}{(1-\xi_1)},$$

where M_S is the eigenvalue of the interacting pair (2,3): $M_S^2 = 4(m^2 + m\epsilon_{23})$ and take into account the interaction between the two particles.

LF description for ^3He

The LF momentum of the free nucleon:

$$\kappa_1^+ = \xi_1 \mathcal{M}_0(1,23), \quad \boldsymbol{\kappa}_{1\perp} = \mathbf{p}_{1\perp} - \xi_1 \mathbf{P}_\perp = \mathbf{k}_{1\perp}.$$

The total momentum of the pair (2,3):

$$K_S^+ = (1-\xi_1)\mathcal{M}_0(1,23) \neq K_{23}^+ = (1-\xi_1) M_0(1,2,3),$$

$$\mathbf{K}_{S\perp} = -\boldsymbol{\kappa}_{1\perp} = -\mathbf{k}_{1\perp} = \mathbf{k}_{2\perp} + \mathbf{k}_{3\perp}.$$

$P_{int}^+(1,23) = \mathcal{M}_0(1,23) \rightarrow P_{int}^+(1,2,3) = M_0(1,2,3)$ boost LF [15].

[15] A. Del Dotto, E. Pace, G. Salmé, S. Scopetta, Phys. Rev. C **95**, 01400 1-22 (2017).

SSFs g_1 and g_2

So, the expression for the SSFs for the ^3He nucleus, in more detail, is given by the convolution equation:

$$g_i^3(x) = \frac{m}{M_3} \sum_{N=n,p} \int_{xm/M_3}^1 \frac{d\xi}{\xi^2} \mathcal{L}_N(\xi)\, g_i^N(z) \;=\; g_i^{3,n} + 2\, g_i^{3,p}$$

with $z = xm/(M_3\xi)$ e $i = 1, 2$.

g_i^N: SSFs for a free nucleon,

$\mathcal{L}_\mathcal{N}$: spin-dependent Light-Front momentum distribution that takes into account nuclear effects.

$$\begin{cases} f_N: & \text{not polarized} \\ l_N: & \text{longitudinal pol.} \\ h_N: & \text{transverse pol.} \end{cases}$$

For numerical calculation reasons, $\mathcal{L}_N$ is expressed in terms of the TMDs:

1. $$\text{TMD}(\xi, k_\perp) \propto \not\int d\epsilon \mathcal{P}^N(\epsilon, \xi, k_\perp)$$
2. $$\mathcal{L}_N(\xi) \propto \int d^2 k_\perp TMD(\xi, k_\perp)$$

In the Bjorken limit:

$$g_1^A(x,Q^2) = \frac{m\ 2\pi}{M_A}\sum_N \int k_\perp dk_\perp \int_{\xi_{min}}^1 d\xi\ \frac{1}{\xi^2}\ \Big\{g_1^\tau(z,Q^2) \times\left[\Delta f^\tau(\xi,k_\perp^2)\left(\frac{p_z}{m}+1+\frac{p_z^2}{m(p^0+m)}\right)+h_{1L}^{\perp\tau}(\xi,k_\perp^2)\ \frac{k_\perp^2}{M_A\ m}\left(1+\frac{p_z}{(p^0+m)}\right)\right]\Big\}$$

with:

$$p_z = \frac{1}{2}\left[(\xi-1)\ M_A + \frac{(A-1)^2m^2+|\mathbf{k}_\perp|^2}{M_A\ (1-\xi)}\right],$$

$$p_0 = \frac{1}{2}\left[(\xi-1)\ M_A + \frac{(A-1)^2m^2-|\mathbf{k}_\perp|^2}{M_A\ (1-\xi)}\right].$$

$$g_2^A(x,Q^2) = \frac{m\ 2\pi}{M_A}\ \sum_N\ \int k_\perp dk_\perp \int_{\xi_{min}}^1\ d\xi\ \frac{1}{\xi^2}\ \Big\{ g_1^\tau(z,Q^2)$$

$$\times \Bigg\{ \Bigg[\Delta'_T f^\tau(\xi,k_\perp^2) + \frac{k_\perp^2 \left(\Delta'_T f^\tau(\xi,k_\perp^2) + \frac{k_\perp^2}{2M_A^2} h_{1T}^{\perp\tau}(\xi,k_\perp^2) \right)}{2m(p^0+m)} + \frac{k_\perp^2\ p_z\ g_{1T}^\tau(\xi,k_\perp^2)}{M_A m(p^0+m)} \Bigg]$$

$$- \left[\Delta f^\tau(\xi,k_\perp^2) \left(\frac{p_z}{m} + 1 + \frac{p_z^2}{m(p^0+m)} \right) + h_{1L}^{\perp\tau}(\xi,k_\perp^2)\ \frac{k_\perp^2}{M_A m} \left(1 + \frac{p_z}{(p^0+m)} \right) \right] \Bigg\}$$

$$+\ g_2^\tau(z,Q^2)$$

$$\times \Bigg[\Delta'_T f^\tau(\xi,k_\perp^2) + \frac{k_\perp^2 \left(\Delta'_T f^\tau(\xi,k_\perp^2) + \frac{k_\perp^2}{2M_A^2} h_{1T}^{\perp\tau}(\xi,k_\perp^2) \right)}{2\ m} \left(\frac{1}{(p^0+m)} - \frac{1 + \frac{p_z}{(p^0+m)}}{p^+} \right)$$

$$+\ \frac{1}{2M_A}\ k_\perp^2\ g_{1T}^\tau(\xi,k_\perp^2) \left(\frac{p_z}{m(p^0+m)} - \frac{\frac{p_z}{m} + 1 + \frac{p_z^2}{m(p^0+m)}}{p^+} \right) \Bigg] \Bigg\}.$$

Numerical calculation of SSFs

The integrals in ξ and in $k_\perp$ were numerically computed using a Fortran program:

- For the TMDs we used the values calculated in Ref. [16] along with the ^3He WF given by A. Kievsky and M. Viviani [17] and the Argonne potential v_{18} (AV18) [18].
- For g_1 we used the parametrization by M. Glück, E. Reya, M. Stratmann, and W. Vogelsang [19],
- For g_2 we used the approximation the Wandzura-Wilczek expression [20]:

$$g_2^{WW}(x) = -g_1(x) + \int_x^1 \frac{dy}{y} g_1(y). \tag{4}$$

[16] R. Alessandro, A. Del Dotto, E. Pace ,G. Perna ,G. Salmè, S. Scopetta, Phys. Rev. C **104**, 065204 (2021).

[17] A. Kievsky, S. Rosati, M. Viviani, Nucl. Phys. A **551**, 241-254, (1993).

[18] R. B. Wiringa, V. G. J. Stoks, R. Schiavilla, (1995).

[19] M. Glück, E. Reya, M. Stratmann, W. Vogelsang, Phys. Rev. D (2001).

[20] A. Harindranath and Wei-Min Zhang, Phys.Lett. B 408 347-356 (1997).